Computational Investigation and Hydrogen/Deuterium Exchange of the Fixed Charge Derivative Tris(2,4,6-Trimethoxyphenyl) Phosphonium: Implications for the Aspartic Acid Cleavage Mechanism

Kristin A. Herrmann and Vicki H. Wysocki
Department of Chemistry, University of Arizona, Tucson, Arizona, USA

Erich R. Vorpagel
Pacific Northwest National Laboratories, Richland, Washington, USA

Aspartic acid (Asp)-containing peptides with the fixed charge derivative tris(2,4,6-trimethoxyphenyl) phosphonium (tTMP-P^+) were explored computationally and experimentally by hydrogen/deuterium (H/D) exchange and by fragmentation studies to probe the phenomenon of selective cleavage C-terminal to Asp in the absence of a "mobile" proton. Ab initio modeling of the tTMP-P^+ electrostatic potential shows that the positive charge is distributed on the phosphonium group and therefore is not initiating or directing fragmentation as would a "mobile" proton. Geometry optimizations and vibrational analyses of different Asp conformations show that the Asp structure with a hydrogen bond between the side-chain hydroxy and backbone carbonyl lies 2.8 kcal/mol above the lowest energy conformer. In reactions with D_2O, the phosphonium-derived doubly charged peptide $(H^+)P^+$L**D**IFS**D**F rapidly exchanges all 12 of its exchangeable hydrogens for deuterium and also displays a nonexchanging population. With no added proton, P^+L**D**IFS**D**F exchanges a maximum of 4 of 11 exchangeable hydrogens for deuterium. No exchange is observed when all acidic groups are converted to the corresponding methyl esters. Together, these H/D exchange results indicate that the acidic hydrogens are "mobile locally" because they are able to participate in exchange even in the absence of an added proton. Fragmentation of two distinct $(H^+)P^+$L**D**IFS**D**F ion populations shows that the nonexchanging population displays selective cleavage, whereas the exchanging population fragments more evenly across the peptide backbone. This result indicates that H/D exchange can sometimes distinguish between and provide a means of separation of different protonation motifs and that these protonation motifs can have an effect on the fragmentation. (J Am Soc Mass Spectrom 2005, 16, 1067–1080) © 2005 American Society for Mass Spectrometry

Proteomics currently relies largely on tandem mass spectrometry (MS/MS) to identify proteins in complex mixtures [1]. Although single stage identification involving mass analysis of in-gel digestion products of gel-separated proteins is still used, many identifications are accomplished via protein digestion followed by on-line peptide separation and MS/MS [2-4]. In this scheme, a protein is subjected to enzymatic digestion and the resulting peptides are separated by high-performance liquid chromatography (HPLC) followed immediately by on-line MS/MS. Ionization is accomplished typically by electrospray ionization (ESI) [5], a technique compatible with on-line HPLC. Peptides are mass selected sequentially and fragmented via collision-induced dissociation (CID). The resulting MS/MS spectra generated are too numerous to manually interpret, so protein identification is typically made through the use of protein or nucleotide sequence database searching programs such as SEQUEST (Thermo Finnigan, San Jose, CA) [6] and Mascot (Matrix Sciences, London, UK) [7]. These programs automatically match experimentally obtained MS/MS data from protein digest products with theoretically generated

Published online May 25, 2005
Address reprint requests to Vicki H. Wysocki, Department of Chemistry, University of Arizona, 1306 East University Boulevard, Tucson, AZ 85721-0041, USA. E-mail: vwysocki@u.arizona.edu

1044-0305/05/$30.00
doi:10.1016/j.jasms.2005.03.028

Received December 1, 2004
Revised March 25, 2005
Accepted March 25, 2005

spectra or peak lists [8]. In this approach, it is presumed that the most likely cleavages occur at the amide bonds along the peptide backbone. If the charge remains on the N-terminal side of the peptide, the product ion is termed b_n, where n refers to the number of amino acid residues counting from the N-terminus. Likewise, if the charge remains on the C-terminal side of the peptide, the fragment is identified as a y_n ion, where n is determined by counting amino acid residues from the C-terminus [9]. Differences between the m/z values of adjacent fragment ions of the same series (e.g., b_n or y_n ions) can be correlated to the mass of an amino acid residue. Database searching can accommodate post-translational modification of peptides by allowing specific, user-defined modifications [10, 11]. If a complete ion series is present, the entire peptide sequence may be determined de novo without a database [12, 13]. This approach is useful for proteins from unsequenced genomes. A partial ion series also can be used in conjunction with database searching. In this mass tag scheme, a partial sequence and the peptide molecular weight are matched to the correct sequence from a database [13-15]. Identified peptides are matched against theoretical protein digests to identify the protein.

Automated, high-throughput identification of proteins by MS/MS and database sequencing algorithms is successful for many samples [1, 3, 4, 8, 12–17], but this approach sometimes fails to identify the protein because of inaccurate algorithm prediction [18]. Statistical [19–24] and mechanistic [25–32] analyses have led to a better understanding of peptide fragmentation behavior. Specifically, these studies have revealed residue-specific preferential cleavage N-terminal to proline (Pro), C-terminal to aspartic acid (Asp) and glutamic acid (Glu), and C-terminal to oxidized cysteine (e.g., cysteine sulfinic acid and cysteine sulfonic acid) [19, 20, 33–43]. The dominance of these preferential cleavages may lead to a loss of fragmentation information because other fragment peaks may be of very low intensity or not present. Incorporation of statistical intensity information and fragmentation "rules" into sequencing algorithms for the generation of theoretical fragmentation spectra may improve identification when matched against the experimental spectra. However, it is also important to understand mechanistically preferential cleavages so their occurrence can be more intelligently predicted. The prediction of low-energy CID spectra based on the kinetics of fragmentation and the "mobile proton" model recently has been reported [44].

The preference of Asp to cleave on its C-terminal side is statistically more prominent when the number of ionizing protons does not exceed the number of basic residues (e.g., arginine and lysine) present in the peptide and is especially prominent for arginine [30, 41, 45]. This observation is significant because the enzyme trypsin is commonly used to digest proteins, leading to a considerable number of arginine- and lysine-containing peptides that are analyzed for identification by tandem mass spectrometry. Selective cleavage data suggest fragmentation C-terminal to Asp occurs without the involvement of the ionizing proton because when the number of ionizing protons does not exceed the number of basic residues (e.g., the proton is sequestered at a basic side-chain) cleavage at Asp is preferentially observed. When a "mobile" proton is available, cleavage is nonselective with many cleavages observed along the peptide backbone.

The phenomenon of selective cleavage C-terminal to Asp in the absence of a mobile proton was investigated previously by attaching the fixed charge tris(2,4,6-trimethoxyphenyl) phosphonium (tTMP-P^+) group to the N-terminus of Asp-containing peptides [34]. A tTMP-P^+ derivatized peptide contains a positively charged tetrahedral phosphorus atom, eliminating the need for an ionizing proton to charge the peptide for mass spectrometric analysis. Cleavages along the peptide backbone will therefore take place without the influence of an ionizing proton. In addition, tTMP-P^+ is a bulky derivative, with charge anticipated as centered at phosphorus, which is not expected to interact significantly with an Asp residue on the attached peptide. Selective cleavage C-terminal to Asp is observed when the fixed charge derivative is present without an ionizing proton. However, when a proton is added making the overall charge state of the derivatized peptides positive two (+2), additional nonselective cleavages along the peptide backbone are prominent [34]. In addition, the fragmentation of a peptide derivatized with tTMP-P^+ is experimentally similar to the fragmentation of the same peptide with the tTMP-P^+ moiety replaced by an arginine and an ionizing proton [34] (i.e., the proton is sequestered at the basic arginine residue). Therefore, it is presumably not necessary for the charged arginine to interact directly with the acidic residue to accomplish fragmentation. Fragmentation C-terminal to acidic residues in the absence of a "mobile" proton can then be considered to occur without the direct influence of the ionizing charge.

In the previously proposed Asp cleavage mechanism shown in Scheme **1** [34, 38], there is a hydrogen bond between the carboxylic acid hydrogen on the acidic side-chain and the adjacent backbone carbonyl oxygen (or perhaps the backbone nitrogen) on the C-terminal side of the peptide.

This interaction makes the backbone carbonyl carbon more susceptible to nucleophilic attack. However, it is unclear whether the hydroxy or carboxy oxygen on the acidic side-chain acts as the nucleophile (shown in Scheme **1** as the hydroxyl oxygen) or whether proton transfer to the amide nitrogen might occur instead, perhaps with assistance from an adjacent carbonyl, as shown in a recent publication [46]. On nucleophilic attack, a five-membered anhydride ring structure is formed that decomposes to the anhydride b-ion structure. The Asp acidic hydrogen can be considered mobile "locally" in this mechanism because it is transferred to the backbone carbonyl or amide nitrogen during formation of the anhydride b-ion. This anhydride b-ion differs from the "typical" b-ion structure formed when a

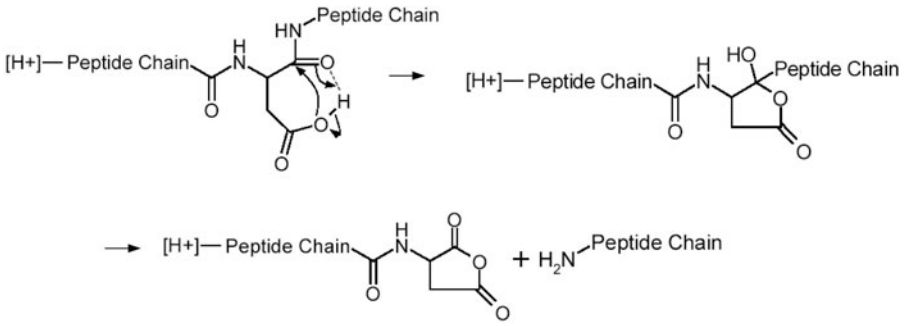

Scheme 1

backbone carbonyl oxygen attacks an electropositive backbone carbonyl carbon to form a protonated oxazalone structure [47-52], as shown Scheme **2**.

Protonation at the amide nitrogen is shown in Scheme **2** for simplicity, although in reality protonation at the carbonyl oxygen and subsequent proton transfer to the nitrogen may occur [46].

Hydrogen/deuterium (H/D) exchange in the gas-phase with D_2O is one method of studying the Asp cleavage mechanism because it provides an indication of the availability of a proton. Therefore, H/D exchange reactions can be used to gauge the *possibility* of intramolecular transfer to another peptide site in the absence of D_2O. However, it is important to note that H/D exchange reactions should be used in *conjunction* with other mechanistic studies because of the possibility of an inserted D_2O molecule significantly altering the gas-phase peptide structure [53]. Mass spectrometry is well suited for the detection of deuterium uptake because the analyte peak shifts by one mass unit for each deuterium incorporated (for +1 charge state). H/D exchange with D_2O or CD_3OD as the exchange reagent is commonly accepted to proceed via the relay mechanism [54, 55]. In this mechanism, the exchange reagent forms a complex with the peptide and a proton is transferred to the exchange reagent while a deuteron is transferred to a separate site on the peptide. Exchange is dependent on the steric availability of the exchanging proton, the basicity difference between the two sites of exchange, the conformational accessibility of the two sites of exchange, and the identity of the exchange reagent [54]. Presumably, deuterium uptake will not occur in the absence of an ionizing proton to act as the exchanging proton unless there exists an acidic hydrogen in the peptide able to transfer to a site of similar basicity.

After publication of the original work studying fixed charge Asp-containing peptides [34], some members of the scientific community questioned whether the positive charge on the tTMP-P^+ moiety might be influencing the site of selective cleavage. The approach of this study is to provide additional evidence through ab initio calculations that the tTMP-P^+ derivative does not interact with the Asp residues. Also, Asp conformations that could potentially lead to selective cleavage are explored computationally. Experimental evidence is presented that acidic hydrogens participate in H/D exchange and can therefore initiate fragmentation even in the absence of an added proton.

Experimental

Molecular Modeling

Computational modeling studies were undertaken at the Molecular Science Computing Facility (MSCF) located at Pacific Northwest National Laboratories (PNNL) on a high-performance Hewitt Packard Linux-based computer containing 980 nodes/1960 Itanium-2 processors. Ab initio calculations were undertaken with the NWChem [56] program along with the Extensible Computational Chemistry Environment [57] graphical interface (Pacific Northwest National Laboratory [PNNL], Richland, WA), both developed at PNNL. All geometry optimizations, vibrational analyses, and electrostatic potential (ESP) calculations used the Dunning-Hay double-ζ basis set [58] with polarization functions added to all atoms [59]. In addition, all calculations except the geometry optimization for tTMP-P^+-(CH_2CO)-AlaAsp-($NHCH_3$) used Hartree-Fock self-consistent-field theory. tTMP-P^+-(CH_2CO)-AlaAsp-($NHCH_3$) was optimized by using density functional

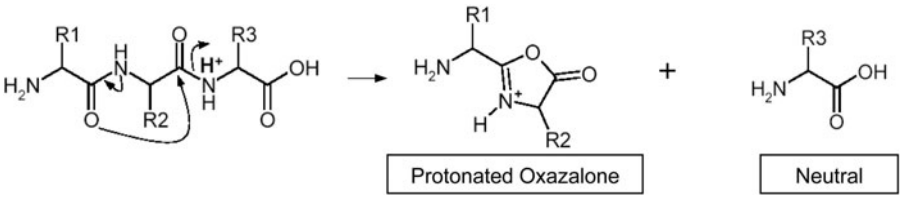

Scheme 2

theory [60, 61] and the hybrid B3LYP exchange-correlation function [62, 63].

In this study, the symbolism TMP-P^+ represents 2,4,6-trimethoxyphenyl phosphonium, tTMP-P represents tris(2,4,6-trimethoxyphenyl) phosphonium, and tTMP-Si represents tris(2,4,6-trimethoxyphenyl) silane. Geometry optimization and vibrational analyses were performed on TMP-P^+H_3 (Figure 1a), tTMP-P^+-CH_3 (Figure 1b), tTMP-Si-CH_3 (Figure 1c), and CH_3CO-(Asp)-$NHCH_3$ (Figure 1d). Partial atomic charge distributions using the restrained ESP [64, 65] method were applied to tTMP-P^+-CH_3 and tTMP-Si-CH_3 to ascertain the location of the positive charge. Vibrational frequencies were calculated to confirm that the geometries were minima on the potential energy surface. Because of its size, only a geometry optimization was performed for tTMP-P^+-(CH_2CO)-AlaAsp-($NHCH_3$) (Figure 1e).

Synthesis

For simplicity, the symbolism P^+ represents the fixed charge derivative tTMP-P^+ when a -CH_2CO- group is used to attach the central phosphorus to a peptide chain. The peptide P^+L**D**IFS**D**F (where L is leucine, D is Asp, I is isoleucine, F is phenylalanine, and S is serine) was prepared by using solid-phase synthesis protocols and was reported previously [34]. 9-Fluoroenylmethoxy-carbonyl (Fmoc) derivatives of the amino acids were purchased from Advanced Chemtech (Louisville, KY). The first residue (C-terminal residue of the finished peptide) was purchased bound to the Wang resin, from Calbiochem/Novabiochem (San Diego, CA). All other reagents required during synthesis were from Sigma-Aldrich (St. Louis, MO).

Acidic groups were converted to the methyl ester form by adding 50–100 μL of 1 M of acetyl chloride in anhydrous MeOH to a small amount of the solid. This reaction results in a mixture of P^+L**D**IFS**D**F, P^+L**D**IFS**D**F$(OMe)_1$, P^+L**D**IFS**D**F$(OMe)_2$, and P^+L**D**IFS**D**F$(OMe)_3$, where $(OMe)_n$ indicates the number of acidic groups converted to the methyl ester form. For the formation of P^+L**D**IFS**D**F$(OMe)_1$ and P^+L**D**IFS**D**F$(OMe)_2$, the location(s) and heterogeneity of the methyl ester(s) are not controlled during the reaction.

Fourier Transform Ion Cyclotron Resonance H/D Exchange and Fragmentation Studies

The model peptide L**D**IFS**D**F has been used previously to study the selective cleavage of Asp in the presence and absence of a fixed charge derivative and/or an arginine residue [34]. Here, we continue these studies with fragmentation and/or H/D exchange data of P^+L**D**IFS**D**F, $(H^+)P^+$L**D**IFS**D**F, P^+L**D**IFS**D**F$(OMe)_1$, $(H^+)P^+$L**D**IFS**D**F$(OMe)_1$, P^+L**D**IFS**D**F$(OMe)_2$, $(H^+)P^+$L**D**IFS**D**F$(OMe)_2$, and P^+L**D**IFS**D**F$(OMe)_3$, where (H^+) indicates an added proton leading to an overall charge state of positive two (+2).

Ions were generated using an Analytica (Branford, CT) second generation electrospray (ESI) source. An IonSpec (Lake Forest, CA) 4.7-tesla Fourier transform ion cyclotron resonance (FT-ICR) instrument was used for H/D exchange and fragmentation studies. A pulsed-leak configuration described by Freiser and coworkers [66] was incorporated to allow a constant reagent gas pressure in the analyzer region for the desired exchange time. D_2O (99.9%) was purchased from Cambridge Isotope Laboratories (Andover, MA)

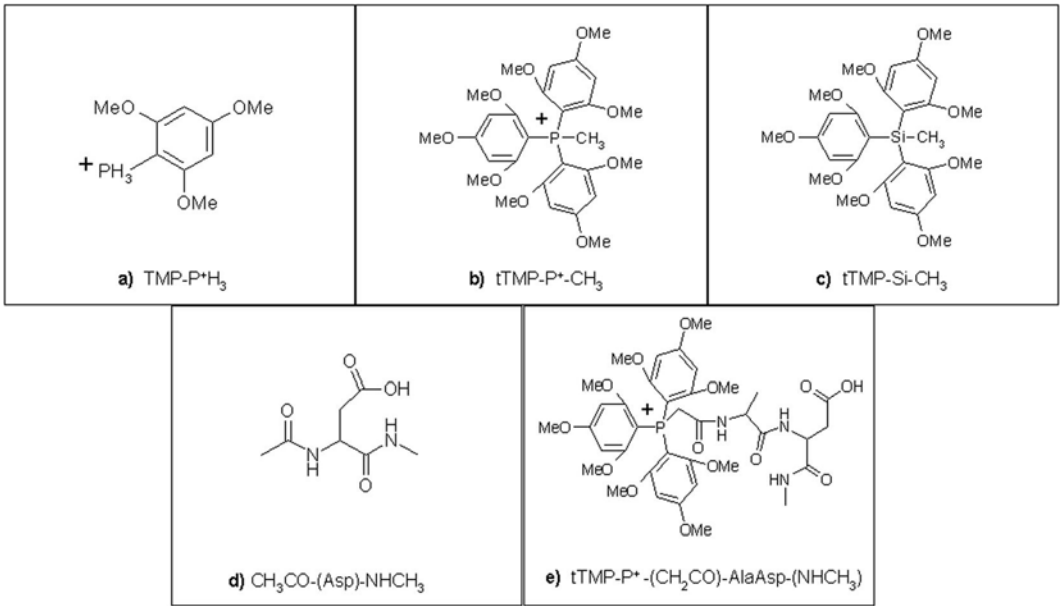

Figure 1. Structures of (**a**) tTMP-P^+H_3, (**b**) tTMP-P^+-CH_3, (**c**) tTMP-Si-CH_3, (**d**) CH_3CO-(Asp)-$NHCH_3$, and (**e**) tTMP-P^+-(CH_2CO)-AlaAsp-($NHCH_3$).

and was degassed through several freeze-thaw cycles before use.

The ions were introduced into the instrument by infusing 10–30 μM solutions of the peptides in 50:50 methanol:water with 1% acetic acid using a stainless steel microelectrospray needle (0.004-in. i.d.) at a flow rate of 2-3 μL/min. The source temperature was kept at 180–200 °C, and 3.8 kV was applied to the electrospray needle. The instrument has two regions of differential cryogenic pumping, referred to as the source and analyzer regions, with a typical analyzer base pressure of 7×10^{-11} torr. The electrosprayed ions pass through a skimmer and are collected in an external rf-only hexapole, where they are allowed to accumulate for 400 ms before being passed into the analyzer through a shutter. An rf-only quadrupole guides the ions into the cylindrical ICR cell. Once the ions were trapped inside the ICR cell, some mass-to-charge values were ejected from the cell via a chirp frequency sweep isolating the desired ion range. Ions were allowed to exchange over a time range of 0–10 min with a constant D_2O pressure. After the appropriate exchange time, a 30-s pump down time was applied to remove neutral reagents and achieve the low pressures necessary for FT-ICR analysis. One to 10 transients were averaged depending on the strength of the ICR signal.

The H/D exchange of P^+L**D**IFS**D**F, P^+L**D**IFS**D**F$(OMe)_1$, P^+L**D**IFS**D**F$(OMe)_2$, and P^+L**D**IFS**D**F$(OMe)_3$ was performed simultaneously with a D_2O pressure of 6×10^{-7} torr. Pressure in the ICR at the time of detection was approximately 2×10^{-8} torr. To maximize the signal, the ions were not monoisotopically selected before reaction with D_2O. The H/D exchange of the doubly charged ion $(H^+)P^+$L**D**IFS**D**F was performed at a lower D_2O pressure of 7×10^{-8} torr. Pressure in the ICR cell at the time of detection was approximately 6×10^{-9} torr. In this case, monoisotopic selection of the precursor ion was used because enough signal was available because of the lower reagent pressure. Heating of the ions occurs on monoisotopic selection, causing some fragmentation when the reagent gas is leaked into the ICR cell. It is assumed the remaining precursor ions are collisionally cooled after several seconds of interaction with the D_2O.

The first apparent rate constant was calculated by assuming pseudo-first-order kinetics because the exchange reagent is considered to be in great excess of the analyte. When applicable, spectra were isotopically corrected based on natural isotopic abundance. Although the instrument was not preconditioned with the deuterating agent, isotopic purity was measured with betaine, a compound with one exchangeable hydrogen and a known rate constant [54]. The exchange of betaine with D_2O was >90% complete, and so contamination and back-exchange were considered negligible. Subsequent apparent rate constants were estimated by the peaks in the exchange time plots where product formation and depletion rates are equivalent [54]. Exchange reagent pressure was corrected for ion gauge sensitivity for the water reagent [67] and the ion gauge (Granville-Phillips, Bayard-Alpert type, Helix Technology Corporation, Mansfield, MA) was calibrated using the H/D exchange reaction of betaine.

Fragmentation of singly charged P^+L**D**IFS**D**F and P^+L**D**IFS**D**F$(OMe)_3$ was accomplished via sustained off resonance irradiation (SORI) CID with argon as the collision gas. The length and amplitude of the SORI pulse was 1000 ms and 5 V, respectively. Doubly charged $(H^+)P^+$L**D**IFS**D**F$(OMe)_1$ and $(H^+)P^+$L**D**IFS**D**F$(OMe)_2$ were fragmented by SORI-CID (SORI time equaled 1000 ms, SORI amplitude equaled 2 V) with nitrogen as the collision gas. Fragmentation of the derivatized peptide P^+L**D**IFS**D**F with one or two deuteriums incorporated was also attempted. The molecular ion was first monoisotopically selected and subjected to H/D exchange for a period of 60 s with CD_3OD as the exchange reagent. Methanol, rather than water, was used as the exchange reagent because the derivatized peptide reacts faster with methanol and therefore the signal is maximized. After H/D exchange, the ion corresponding to incorporation of either one or two deuteriums was monoisotopically selected and then fragmented via SORI-CID with argon as the collision gas. Unfortunately, fragmentation of the exchanged modified peptides showed scrambling of the deuteriums and therefore determining the site of preferred deuterium incorporation was not possible.

Two distinct $(H^+)P^+$L**D**IFS**D**F ion populations were formed on H/D exchange and fragmented via SORI-CID. In this case, the precursor ion was not monoisotopically selected to obtain enough signal for the subsequent H/D exchange, isolation, and fragmentation steps. The precursor ion was subjected to H/D exchange for 30 s with a D_2O pressure of 7×10^{-8} torr. After 30 s of H/D exchange, the two ion populations that emerged were separated by three mass-to-charge units, and so monoisotopic selection of each ion population was not performed to preserve signal intensity. The nonexchanging population was isolated along with its three most abundant carbon-13 isotope peaks. The exchanging population corresponding to 6 through 11 deuteriums incorporated plus corresponding carbon-13 isotope peaks were isolated as a group. The nonexchanging and exchanging ion populations were each isolated and fragmented by SORI-CID (SORI time equaled 500 ms; SORI amplitude equaled 3.5 V) with argon as the collision gas.

Ion Trap H/D Exchange

The derivatized peptides P^+L**D**IFS**D**F and P^+L**D**IFS **D**F$(OMe)_3$ were subjected to H/D exchange with D_2O in a ThermoFinnigan ESI-quadrupole ion trap (QIT). H/D exchange in the QIT is complementary to FT-ICR exchange because the QIT exchange reagent pressure is about four orders of magnitude greater, although exchange time is practically limited to less than a minute. The instrument was modified to

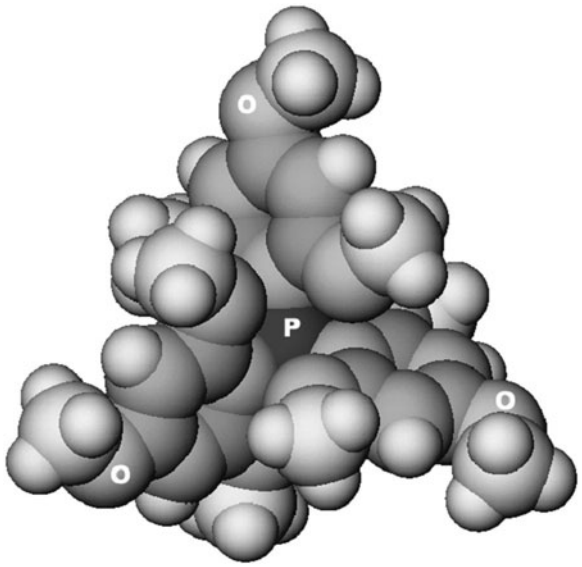

Figure 2. ESP results for tTMP-P^+-CH_3. Darker shades of grey indicate a larger positive charge. The largest positive charge is 1.55 and the largest negative charge is −0.93.

accommodate H/D exchange reactions as described by Gronert [68]. In this system, D_2O is mixed with the helium flow gas and introduced into the instrument. Peptide solutions (~50 μM) in 50:50 methanol:water with 1% acetic acid were infused into the instrument at a flow rate of 8 μL/min. The instrument was first conditioned with D_2O for approximately 1 h to remove any hydrogen contamination. The desired ion was isolated and allowed to exchange for up to 40 s at a D_2O reagent pressure of approximately 10^{-3} torr. The 40-s exchange time was achieved with four sequential 10-s isolations of the exchanging compound. Each 40-s exchange experiment was repeated 10 times and the spectra were averaged.

Results and Discussion

Fixed Charge Derivative: ESP

To determine if the tTMP-P^+ derivative is electrostatically influencing the fragmentation site (e.g., interacting with the acidic side-chain or the adjacent backbone carbonyl), an ab initio calculation of the tTMP-P^+ derivative ESP was performed. Presumably, if the majority of the positive charge on the tTMP-P^+ fixed charge derivative is localized, then this positive charge will not directly influence the fragmentation site.

A geometry optimization and vibrational analysis was first performed for TMP-P^+H_3 (Figure 1a), which represents the simplest unit of the tTMP-P^+ derivative. The results show the three methoxy groups in the plane of the phenyl ring in the lowest energy conformation. The conformation with the methoxy group *para* to the phosphorus atom perpendicular to the phenyl ring is 5 kcal/mol higher in energy. The starting structure of tTMP-P^+-CH_3 (Figure 1b) was constructed from the results of the geometry optimization for TMP-P^+H_3. Terminating tTMP-P^+ with CH_3 simplifies the ab initio geometry optimization of this large molecule because the molecule possesses C_3 symmetry. A geometry optimization and vibrational analysis was calculated for tTMP-P^+-CH_3, and the isoelectric neutral molecule tTMP-Si-CH_3 (Figure 1c).

The ESP for tTMP-P^+-CH_3 is shown in Figure 2, with the largest positive charge, 1.55, shaded the darkest and the largest negative charge, −0.93, shaded the lightest.

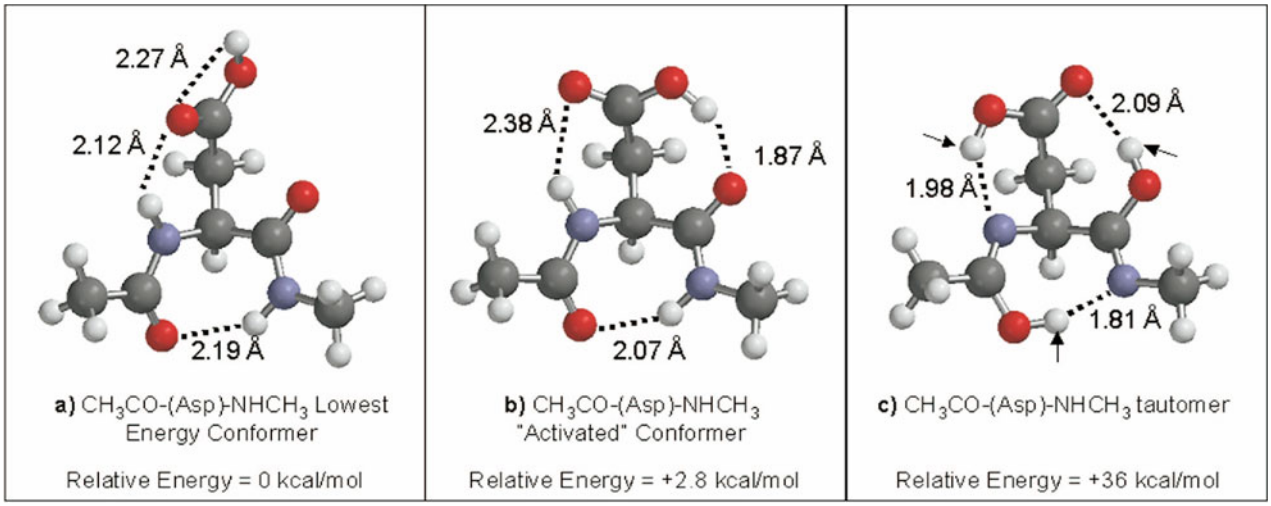

Figure 3. Geometry optimized structures for CH_3CO-(Asp)-$NHCH_3$ conformers, shown along with hydrogen bonding distances: (**a**) lowest energy conformer with relative energy 0 kcal/mol, (**b**) activated conformer with a relative energy of +2.8 kcal/mol, and (**c**) tautomer structure with a relative energy of +36 kcal/mol (arrows indicate protons that have migrated relative to the lowest energy and activated conformers).

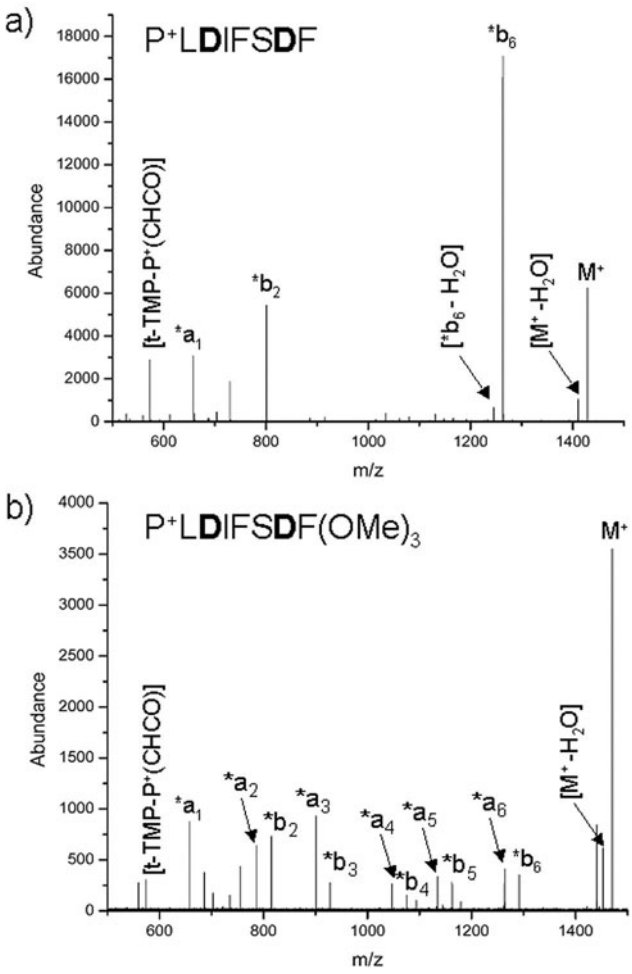

Figure 4. FT-ICR SORI-CID fragmentation spectra with argon as the collision gas. SORI time equals 1000 ms, SORI amplitude equals 5V. (**a**) P^+L**D**IFS**D**F and (**b**) P^+L**D**IFS**D**F$(OMe)_3$.

This result verifies that the positive charge is distributed within the *t*-TMP$^+$P derivative near the formally charged phosphorus atom and alternating carbon atoms in the phenyl rings. Therefore, this positive charge can only influence the cleavage of an Asp on an attached peptide by a through-space electrostatic field effect (i.e., a non-local manner). It is interesting to compare the partial atomic charges for tTMP-P^+-CH_3 with tTMP-Si-CH_3. When phosphorus is replaced with silicon in the fixed charge derivative, the isoelectronic structure is neutral but shows very similar partial atomic charge distribution. The largest difference in the charge between the phosphonium and silane is only two tenths of the unit charge.

Fixed Charge Derivative: Exploring Structural Interactions with Proximal Asp Residue

To provide further evidence that the tTMP-P^+ fixed charge derivative is not likely to directly interact with an Asp residue on an attached peptide chain, a small dipeptide, alanine-Asp (AlaAsp), attached to the fixed charge derivative (Figure 1e) was subjected to a geometry optimization. The peptide AlaAsp was chosen because Asp is two residues away from the fixed charge derivative, the closest separation in previously investigated systems in which selective cleavage was observed C-terminal to Asp in the absence of an ionizing proton (e.g., P^+L**D**IFS**D**F [34]). Ala was chosen as the first residue because its structural simplicity decreases the computational time required. Terminating the N- and C-termini with acetyl and *N*-methyl groups, respectively [i.e., CH_3CO-(Asp)-$NHCH_3$ and tTMP-P^+-(CH_2CO)-AlaAsp-($NHCH_3$)] simulates a continuing peptide chain because through-bond inductive effects become less significant as a function of the number of bonds of separation. A geometry optimization and vibrational analysis was first performed for CH_3CO-(Asp)-$NHCH_3$ (Figure 1d). The lowest energy conformer (Figure 3a) has an internal hydrogen bond between the side-chain carbonyl oxygen and hydroxyl hydrogen. Geometry was optimized for the molecule tTMP-P^+-(CH_2CO)-AlaAsp-($NHCH_3$) by using, for the starting structure, the lowest energy structures calculated for tTMP-P^+-CH_3 and CH_3CO-(Asp)-$NHCH_3$. The result of this calculation shows that the fixed charge does not interact structurally with the attached Asp residue.

Charge-Remote Cleavage: Asp Structures

Ab initio structures of Asp residues were explored to determine the feasibility, both conformationally and energetically, of nucleophilic attack by the Asp carboxy or hydroxy group on the adjacent backbone carbonyl oxygen. As noted in the previous section, the lowest energy structure of Asp has an internal hydrogen bond between the side-chain carbonyl oxygen and side-chain hydroxyl hydrogen (Figure 3a).

The structure in which the side-chain hydroxyl hydrogen forms a hydrogen bond with the adjacent carbonyl oxygen on the peptide backbone was also explored (Figure 3b). This "activated" structure (because its conformation contains the hydrogen bond required for the proposed cleavage mechanism) was found to lie only 2.8 kcal/mol (corrected for zero-point energy) above the "inactivated" structure. Therefore, this activated structure is potentially accessible during the activation event to fragment the molecule (i.e., CID), although the exploration of the transition-state is necessary to be absolutely sure the energy barrier is within the energy regime of a typical mass spectrometry experiment. An Asp tautomer was explored as an alternative structure and is shown in Figure 3c with the arrows indicating protons that have migrated relative to the lowest energy and activated conformers. This structure was found to lie 36 kcal/mol in energy above the lowest energy conformer and 33 kcal/mol above the activated conformer. Although the exploration of the transition states between these conformers is beyond

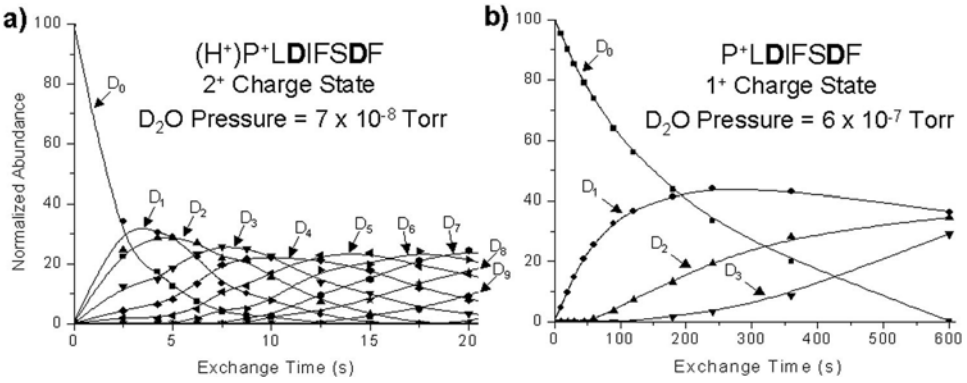

Figure 5. H/D exchange relative abundance curves as a function of time. D_n label indicates the number of deuterium incorporations each curve corresponds to. (**a**) Doubly charged $(H^+)P^+$L**D**IFS**D**F (D_2O pressure equals 7×10^{-8} torr; nine deuteriums incorporated after 20 s of exchange). (**b**) Singly charged P^+L**D**IFS**D**F (D_2O pressure equals 6×10^{-7} torr; three deuteriums incorporated after 600 s of exchange).

the scope of this study, these energy differences represent a lower limit for the energy barrier.

*Fragmentation of P^+L**D**IFS**D**F and P^+LDIFS**D**F(OMe)$_3$*

Figure 4 shows the SORI-CID fragmentation of the derivatized peptides with free acidic groups (P^+L**D**IFS**D**F) and with all acid groups converted to the methyl ester [P^+L**D**IFS**D**F(OMe)$_3$].

In these figures, the notations *b_n and *a_n indicate standard b_n and a_n ions modified with the fixed charge derivative at the N-terminus. As expected, the major *b_n ions formed via fragmentation of P^+L**D**IFS**D**F result from cleavage C-terminal to the Asp residues (i.e., *b_2 and *b_6). By contrast, when all acidic groups are converted to methyl esters, cleavage results in *b_2, *b_3, *b_4, *b_5, and *b_6 ions. Furthermore, the relative abundance of these five *b_n ions is roughly equal. The differential formation of the *b_n ions in the spectra indicates that backbone cleavage is more selective (i.e., fragmentation C-terminal to Asp) in P^+L**D**IFS**D**F with the three acidic groups intact and more random in P^+L**D**IFS**D**F(OMe)$_3$ with the acidic groups blocked.

Another interesting feature of the spectra in Figure 4 is the formation of *a_n ions when the acidic groups have been converted to their methyl ester form. It is commonly accepted that a_n ions form when b_n ions lose CO. The typical b_n ion structure produced when a charge induces cleavage is an oxazalone. This protonated oxazalone forms when a backbone carbonyl oxygen attacks an electropositive backbone carbonyl carbon [47-52] (Scheme **2**). It is not clear what structure the *b_n ions have in the absence of an added proton. The *lack* of *a_n ions observed in Figure 4a indicates the *b_n ions observed by selective cleavage do not have the same *b_n structure as formed from P^+L**D**IFS**D**F(OMe)$_3$ and suggests the ions are forming in a mechanistically different manner.

*Fragmentation of $(H^+)P^+$L**D**IFS**D**F(OMe)$_1$ and $(H^+)P^+$L**D**IFS**D**F(OMe)$_2$*

To investigate the most likely site of methyl ester formation, the doubly charged fixed charge derivative peptides $(H^+)P^+$L**D**IFS**D**F(OMe)$_1$ and $(H^+)P^+$L**D**IFS**D**F(OMe)$_2$ were fragmented via SORI-CID. Competition between "charge-directed" and "charge-remote" mechanisms may be occurring during fragmentation of $(H^+)P^+$L**D**IFS**D**F-(OMe)$_1$ and $(H^+)P^+$L**D**IFS**D**F(OMe)$_2$, and so only an estimate of heterogeneity is possible. Based on the fragmentation of $(H^+)P^+$L**D**IFS**D**F(OMe)$_1$ (data not shown), the preferred site of methyl ester formation is the C-terminus. The ratio of the *b_6 and (*b_6 + 14) ions is approximately 85:15. The *b_2, *b_3, *b_4, *b_5, and corresponding +14 (+OMe) ions were also observed and indicate that the methyl ester formation at the Asp residue closer to the C-terminus is slightly preferred over methyl ester formation at the Asp residue closer to the fixed charge derivative. The *b_6 ion was roughly four times the intensity of the individual *b_2, *b_3, *b_4, and *b_5 ions.

Fragmentation of $(H^+)P^+$L**D**IFS**D**F(OMe)$_2$ (data not shown) results in a (*b_6 + 14) and (*b_6 + 28) ion ratio of approximately 88:12. This suggests a population in which approximately 88% of the ions have the methyl ester formed at the C-terminus and one of the Asp residues. In addition, 12% of the ions have both Asp groups converted to the methyl ester. The *b_2, *b_3, *b_4, *b_5, and corresponding +14 (+OMe) ions agree with the fragmentation of $(H^+)P^+$L**D**IFS**D**F-(OMe)$_1$ by indicating a minor preference for methyl ester formation at the Asp residue closer to the C-terminus over the Asp residue closer to the fixed charge derivative. Also, the *b_6 ion was roughly four times the intensity of the individual *b_2, *b_3, *b_4, and *b_5 ions. The formation of y_n ions was not significant for either $(H^+)P^+$L**D**IFS**D**F(OMe)$_1$ or $(H^+)P^+$L**D**IFS**D**F(OMe)$_2$. Fragmentation spectra of singly charged P^+L**D**IFS**D**F-(OMe)$_1$ and P^+L**D**IFS**D**F(OMe)$_2$ were consistent with

Table 1. H/D exchange rates for modified L**D**IFS**D**F peptides with D_2O as the exchange reagent (rates $\times 10^{12}$ cm^3 mol^{-1} s^{-1}, error estimated at 20% because of uncertainty in ion gauge)

Peptide	Charge state	No. of exchangeable hydrogens	No. of hydrogens exchanged	k_1	k_2	k_3	k_4	k_5	k_6	k_7	k_8	k_9	k_{10}	k_{11}	k_{12}
(H^+)GG [54]	1	5	5	310	520	360	47	7	—	—	—	—	—	—	—
P^+L**D**IFS**D**F	1	11	3[a]	0.097	0.063	—[b]	—	—	—	—	—	—	—	—	—
$(H^+)P^+$L**D**IFS**D**F	2	12	12[c]	76	48	46	39	36	29	23	19	14	7.6	5.9	2.8
P^+L**D**IFS**D**F$(OMe)_1$	1	10	3	0.13	0.046	—[b]	—	—	—	—	—	—	—	—	—
P^+L**D**IFS**D**F$(OMe)_2$	1	9	2	0.061/0.015[d]	—[b]	—	—	—	—	—	—	—	—	—	—
P^+L**D**IFS**D**F$(OMe)_3$	1	8	0	—	—	—	—	—	—	—	—	—	—	—	—

[a] Four exchanges observed in QIT at a higher D_2O pressure.
[b] The nth exchange was not extensive enough to calculate k_n.
[c] Ten percent of the ion population did not exchange on the timescale of the experiment; rate constants are shown for the exchanging population.
[d] Two populations with a different apparent first rate constants were observed.

the C-terminus as the preferred site of methyl ester formation (~80%), and with methyl ester formation at the Asp closer to the C-terminus preferred over the Asp closer to the fixed charge derivative.

*H/D Exchange of P^+L**D**IFS**D**F, $(H^+)P^+$L**D**IFS**D**F, and P^+L**D**IFS**D**F$(OMe)_{1\text{-}3}$ with D_2O*

H/D exchange with D_2O in the gas-phase can be used to *gauge* the "mobility" of a proton and is one method of investigating Asp-containing fixed charge derivative peptides.

Figure 5a shows the normalized abundance curves for deuterium incorporation into $(H^+)P^+$L**D**IFS**D**F as a function of time with D_2O as the exchange reagent at a pressure of 7×10^{-8} torr. The doubly charged phosphonium derivatized peptide exhibits facile exchange with rate constants shown in Table 1.

For comparison, the rate constants previously reported [54] for the D_2O H/D exchange of digycine (GG), a small, rapidly exchanging peptide, are also shown in Table 1. After a 600-s exchange (data not shown), approximately 68% of the $(H^+)P^+$L**D**IFS**D**F ion population has incorporated 12 deuteriums, corresponding to all exchangeable hydrogens replaced by deuterium. In addition to the exchanging population illustrated in Figure 5a, another nonexchanging population exists and is discussed in a later section of this article.

The fixed charge derivative peptides with no additional proton might be expected to not be able to participate in the H/D exchange mechanism because there is not an ionizing proton to shuttle to/from the D_2O exchange reagent. However, the derivatized peptide P^+L**D**IFS**D**F in its free acid form surprisingly exchanges 3 of 11 exchangeable hydrogens for deuterium in 10 min in the FT-ICR with D_2O as the exchange reagent at a pressure of 6×10^{-7} torr (Figure 5b). Apparent rate constants are three orders of magnitude lower than for the exchange of the modified peptide with an added proton (Table 1). This peptide was also subjected to H/D exchange in a QIT instrument, which has a higher reagent pressure (four orders of magnitude) but shorter exchange times (less than one minute). After 40 s of exchange, one additional exchange, for a total of four, was observed (because of the higher reagent pressure, data not shown).

When all three acid groups are converted to the methyl ester, P^+L**D**IFS**D**F$(OMe)_3$, no exchange is observed on the timescale of the FT-ICR experiment (Figure 6) or in the QIT (data not shown).

Presumably, the acidic hydrogens account for the H/D exchange with unblocked acidic groups because forming the methyl esters stops the H/D exchange reaction. The fourth exchange probably occurs at the serine side-chain. However, additional experiments are necessary to unequivocally rule out exchange by the

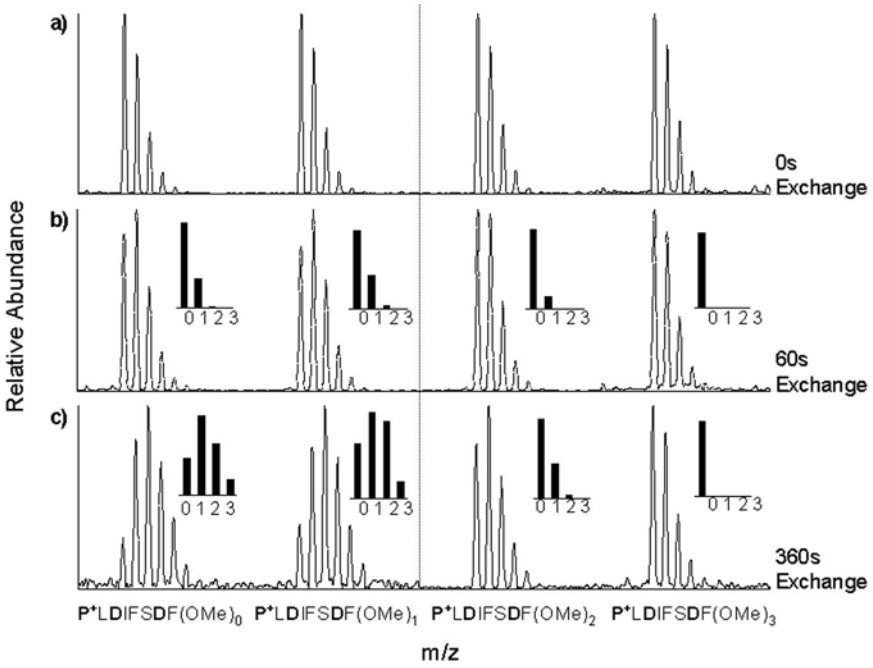

Figure 6. Nonisotopically corrected spectra for the FT-ICR H/D exchange of P^+L**D**IFS**D**F, P^+L**D**IFS**D**F(OMe)$_1$, P^+L**D**IFS**D**F(OMe)$_2$, and P^+L**D**IFS**D**F(OMe)$_3$ with isotopically corrected line spectra shown as insets. The four precursor ions were selected as a group and exchanged with D_2O simultaneously at a reagent pressure of 6×10^{-7} torr. For clarity and because of differences in intensity, each envelope of peaks is normalized to the most abundant peak in that envelope: (**a**) 0 s of exchange, (**b**) 60 s of exchange, and (**c**) 360 s of exchange,

backbone amide groups. Presumably, the unblocked serine side-chain in P^+L**D**IFS**D**F(OMe)$_3$ can not participate in H/D exchange because the acidic groups are blocked and can not act as a partner for the H/D exchange reaction. The lack of H/D exchange of P^+L**D**IFS**D**F(OMe)$_3$ is consistent with the relay mechanism requirement for two partners bridging a proton for exchange.

P^+L**D**IFS**D**F(OMe)$_1$, with one of three acid groups converted to the methyl ester (nonspecifically), displays three exchanges in the FT-ICR (Figure 6) with apparent rate constants shown in Table 1. Because the C-terminus is the preferred site of methyl ester formation (as discussed previously), most of the H/D exchange in this case likely involves the two Asp residues with the third exchange at serine. P^+L**D**IFS**D**F(OMe)$_2$ displays much slower exchange with two exchanges detected after 360 s (Figure 6). Two distinct populations are observed for the first exchange (apparent first rate constants shown in Table 1), which is consistent with the heterogeneity of the methyl ester formation. The fact that no exchange occurs when all three acid groups are blocked and two exchanges occur when only one acid group is unblocked suggests that the exchange mechanism, when no added proton is present, requires interaction between two sites.

Together, these results show that the acidic hydrogens are participating in H/D exchange *in the absence of a mobile ionizing proton*. The H/D exchange at these acidic hydrogens is consistent with the idea that these protons are mobile locally and are potentially able to initiate fragmentation.

*H/D Exchange and Fragmentation of $(H^+)P^+$L**D**IFS**D**F*

As noted previously and as illustrated in Figure 7a, the H/D exchange of $(H^+)P^+$L**D**IFS**D**F results in two ion populations. Furthermore, these ion populations display different fragmentation patterns. Population A, 10% of the total ion abundance, does not display any exchange with D_2O at a pressure of 7×10^{-8} torr and a maximum exchange time of 600 s. Population B, 90% of the total ion abundance, exchanges rapidly on the timescale and pressure of the experiment. Populations A and B were each isolated after 30 s of exchange of $(H^+)P^+$L**D**IFS**D**F with D_2O and fragmented via SORI-CID. Population A was selected along with its three most abundant carbon-13 isotope peaks. Population A displays selective cleavage with fragmentation occurring most prominently C-terminal to the Asp residues forming the $^*b_2$ and $^*b_6$ ions (Figure 7b). Population B, cleanly separated from Population A by three mass-to-charge units after 30 s of H/D exchange, was selected as a group of ions corresponding to 6-11 deuteriums incorporated. The fragmentation of Population B results in regularly spread, fairly uniform cleavage along the entire peptide backbone (Figure 7c). Although the $^*b_6$ ion remains the most abundant fragmentation ion, the

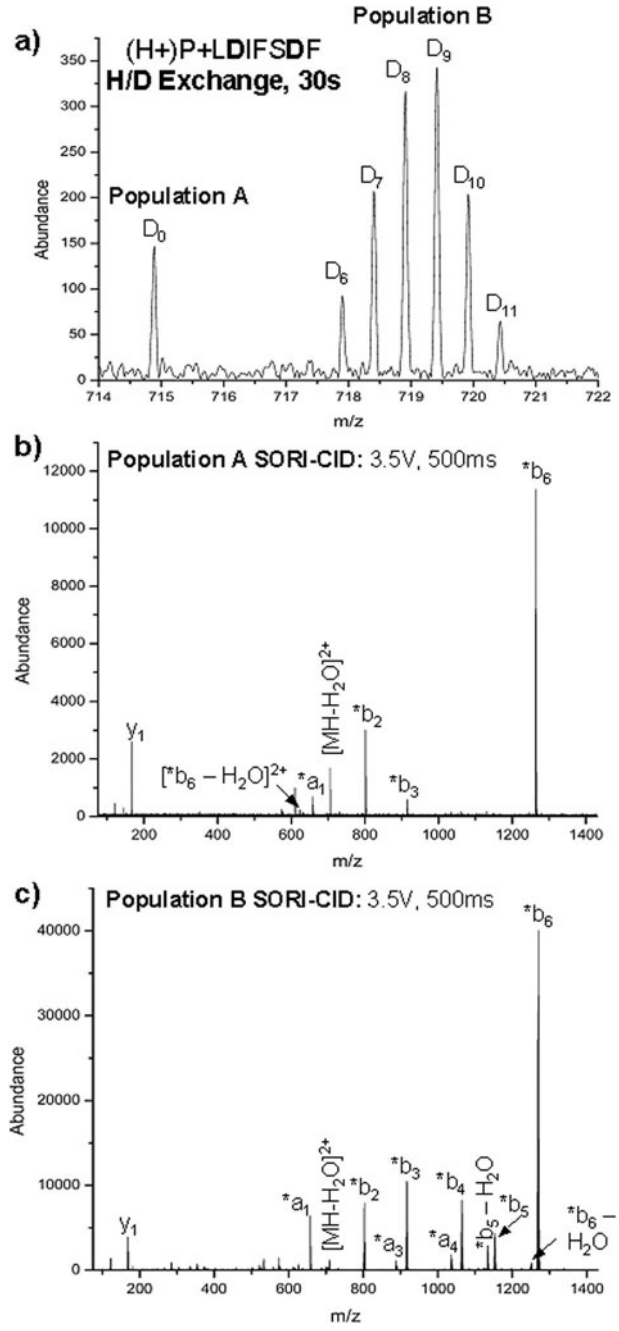

Figure 7. H/D exchange of $(H^+)P^+$L**D**IFS**D**F and fragmentation of the resulting ion populations. (**a**) H/D exchange for 30 s with D_2O after monoisotopic selection of $(H^+)P^+$L**D**IFS**D**F (D_2O pressure equals 7×10^{-8} torr). Population A represents the precursor ion with no deuterium incorporated. Population B represents the precursor ion with 6-11 deuteriums incorporated. (**b-c**) SORI-CID (SORI time equals 500 ms; SORI amplitude equals 3.5V) with argon as the collision gas after nonmonoisotopic selection of $(H^+)P^+$L**D**IFS**D**F (H/D exchange with D_2O at 7×10^{-8} torr for 30 s) and nonmonoisotopic selection of (**b**) Population A (selection and fragmentation of nonexchanging ion along with three nonexchanging carbon-13 isotope peaks). (**c**) Population B (selection and fragmentation of ions corresponding to 6-11 deuteriums incorporated along with exchanged carbon-13 isotope peaks).

$^*a_1$, $^*a_3$, $^*b_3$, $^*a_4$, $^*b_4$, $^*b_5$-H_2O, and $^*b_5$ ions are present at a significant intensity.

No significant isotope effect is expected for cleavage of the deuterated and nondeuterated fixed charge derivative peptides; this was confirmed by taking a linear combination of the fragmentation spectra for Populations A and B and taking into account the percentage of the total ion population (i.e., the fragmentation spectra of Populations A and B were multiplied by 0.1 and 0.9, respectively). The linear combination of these spectra is very similar to the spectrum obtained for the combined population (with no exchange). The fragmentation spectrum of $(H^+)P^+$L**D**IFS**D**F (no exchange) has been previously° published° [34]° and° is° similar° to° that° of Population°B°(Figure°7c).

These results indicate that in the exchanging Population B, the added proton is more mobile and able to initiate charge-directed fragmentation along the peptide backbone. In the nonexchanging Population A, the added proton is more sequestered, and can not initiate charge-directed cleavage. Therefore, charge-remote fragmentation pathways become dominant and $^*b_2$ and $^*b_6$ are the main $^*b_n$ ions observed. The site at which the proton is sequestered is not obvious, but only the singly charged $^*b_2$ and $^*b_6$ ions are formed, suggesting the proton is not located at the fixed charge derivative. A minor peak corresponding to the doubly charged [$^*b_6$ − H_2O] ion is present. Also, the y_1 ion is more dominant in the fragmentation of the nonexchanging population. One possibility is that, in the nonexchanging population, the added proton is solvated by several or all of the oxygen-containing functional groups including the Asp side-chains, the C-terminus, and the serine side-chain.

Conclusions

Ab initio calculations of the fixed charge derivative tTMP-P^+ support its use to investigate the selective cleavage of Asp-containing peptides in the absence of a mobile proton. Calculating partial atomic charges from the ESP of the tTMP-P^+ derivative shows that the positive charge is buried in the center of the bulky derivative. Therefore, tTMP-P^+ can not activate the proposed Asp nucleophile. The possibility of interactions between the tTMP-P^+ derivative and an attached peptide was further investigated by modeling the structure of tTMP-P^+-(CH_2CO)-AlaAsp-($NHCH_3$). The lowest energy structure had no apparent interactions between the fixed charge derivative and the attached dipeptide, providing further evidence that the fixed charge derivative acts as an autonomous unit.

Structural calculations of CH_3CO-(Asp)-$NHCH_3$ provide insight into the cleavage mechanism in the absence of a mobile proton. The calculations of CH_3CO-(Asp)-$NHCH_3$ show that the conformer with a hydrogen bond between the side-chain hydroxyl and the backbone carbonyl is 2.8 kcal/mol higher in energy than the lowest energy conformer, although a transition-state structure is necessary to be absolutely certain the kinetic barrier is

accessible. The possibility of a tautomer structure was also explored. The tautomer structure was 36 kcal/mol above the lowest energy conformer, an energy difference that represents the lower limit for the activation barrier.

Despite the absence of an ionizing proton, the derivatized peptide P^+L**D**IFS**D**F in its free acid form exchanges three hydrogens for deuterium in a FT-ICR mass spectrometer with D_2O as the exchange reagent. One additional exchange is observed using the QIT H/D exchange method with a higher D_2O pressure. However, when all acidic groups are converted to the methyl ester form [e.g., P^+L**D**IFS**D**F$(OMe)_3$], no exchange is observed in either FT-ICR or QIT H/D exchange. This evidence supports the proposed Asp cleavage mechanism that occurs without the direct involvement of an ionizing proton because acidic protons are able to participate in H/D exchange with D_2O and therefore are mobile locally.

Studies of $(H^+)P^+$L**D**IFS**D**F show that at least two distinct structures exist with different H/D exchange behaviors and fragmentation patterns. One population does not exchange any hydrogen for deuterium on the timescale and pressure of the experiment. This population also exhibits selective cleavage C-terminal to the Asp residues, suggesting that the added proton is unavailable to initiate cleavage (not mobile). In addition, the lack of doubly charged ions suggests the location of the sequestered proton is not at the fixed charge derivative. A second population rapidly exchanges hydrogen for deuterium with D_2O. Fragmentation of this exchanging population occurs along the entire peptide backbone, indicating a proton that is mobile and able to initiate charge-directed fragmentation.

Acknowledgments

This research was supported by the National Institutes of Health grant 2 R01 GM051387 to V. H. Wysocki. Computational work was performed under Environmental Molecular Sciences Laboratory (EMSL)-MSCF FY 2003 user proposal 3691 in the EMSL, a national scientific user facility sponsored by the Department of Energy's Office of Biological and Environmental Research and located at PNNL.

References

1. Gavin, A. C.; Bosche, M.; Krause, R.; Grandi, P.; et al. Functional Organization of the Yeast Proteome by Systematic Analysis of Protein Complexes. *Nature* **2002,** *415,* 141–147.
2. Yates, J. R. Database Searching Using Mass Spectrometry Data. *Electrophoresis* **1998,** *19,* 893–900.
3. Link, A. J.; Eng, J.; Schieltz, D. M.; et al. Direct Analysis of Protein Complexes Using Mass Spectrometry. *Nat. Biotechnol.* **1999,** *17,* 676–682.
4. Washburn, M. P.; Wolters, D.; Yates, J. R. Large-Scale Analysis of the Yeast Proteome by Multidimensional Protein Identification Technology. *Nat. Biotechnol.* **2001,** 242–247.
5. Fenn, J. B.; Mann, M.; Meng, C. K.; Wong, S. F.; Whitehouse, C. M. Electrospray Ionization for Mass-Spectrometry of Large Biomolecules. *Science* **1989,** *246,* 64–71.
6. Eng, J. K.; McCormack, A. L.; Yates, J. R. An Approach to Correlate Tandem Mass-Spectral Data of Peptides with Amino-Acid-Sequences in a Protein Database. *J. Am. Soc. Mass Spectrom.* **1994,** *5,* 976–989.
7. Perkins, D. N.; Pappin, D. J. C.; Creasy, D. M.; Cottrell, J. S. Probability-Based Protein Identification by Searching Seqeuence Databases Using Mass Spectrometry Data. *Electrophoresis* **1999,** *20,* 3551–3567.
8. Fenyo, D. Identifying the Proteome: Software Tools. *Curr. Opin. Biotechnol.* **2000,** 391–395.
9. Biemann, K. Contributions of Mass Spectometry to Peptide and Protein Structure. *Biomed. Environ. Mass Spectrom.* **1988**, *16,* 99–111.
10. Yates, J. R.; Eng, J. K.; McCormack, A. L.; Schieltz, D. Method to Correlate Tandem Mass-Spectra of Modified Peptides to Amino-Acid-Sequences in the Protein Database. *Anal. Chem.* **1995,** *67,* 1426–1436.
11. Liebler, D. C.; Hansen, B. T.; Davey, S. W.; Tiscareno, L.; Mason, D. E. Peptide Sequence Motif Analysis of Tandem MS Data with the SALSA Algorithm. *Anal. Chem.* **2002,** *74,* 203–210.
12. Goodlett, D. R.; Keller, A.; Watts, J. D.; Newitt, R.; Yi, E. C.; et al. Differential Stable Isotope Labeling of Peptides for Quantitation and De Novo Sequence Derivation. *Rapid Commun. Mass Spectrom.* **2001,** *15,* 1214–1221.
13. Taylor, J. A.; Johnson, R. S. Sequence Database Searches via De Novo Peptide Sequencing by Tandem Mass Spectrometry. *Rapid Commun. Mass Spectrom.* **1997,** *11,* 1067–1075.
14. Mann, M.; Wilm, M. Error Tolerant Identification of Peptides in Sequence Databases by Peptide Sequence Tags. *Anal. Chem.* **1994,** *66,* 4390–4399.
15. Shevchenko, A.; Sunyaev, S.; Loboda, A.; Shevehenko, A.; et al. Charting the Proteomes of Organisms with Unsequenced Genomes by MALDI-Quadrupole Time of Flight Mass Spectrometry and BLAST Homology Searching. *Anal. Chem.* **2001,** *73,* 1917–1926.
16. Mann, M.; Hendrickson, R. C.; Pandey, A. Analysis of Proteins and Proteomes by Mass Spectrometry. *Ann. Rev. Biochem.* **2001,** *70,* 437–473.
17. Johnson, R .S.; Taylor, J. A. Searching Sequence Databases via De Novo Peptide Sequencing by Tandem Mass Spectrometry. *Mol. Biotechnol.* **2002,** *22,* 301–315.
18. Simpson, R. J.; Connolly, L. M.; Eddes, J. S.; et al. Proteomic Analysis of the Human Colon Carcinoma Cell Line (LIM 1215): Development of a Membrane Protein Database. *Electrophoresis* **2000,** *21,* 1707–1732.
19. Breci, L. A.; Tabb, D. L.; Yates, J. R.; Wysocki, V. H. Cleavage N-Terminal to Proline: Analysis of a Database of Peptide Tandem Mass Spectra. *Anal. Chem.* **2003,** *75,* 1963–1971.
20. Huang, Y. Y.; Wysocki, V. H.; Tabb, D. L.; Yates, J. R. The Influence of Histidine on Cleavage C-Terminal to Acidic Residues in Doubly Protonated Tryptic Peptides. *Int. J. Mass Spectrom.* **2002,** *219,* 233–244.
21. Kapp, E. A.; Schutz, F.; Reid, G. E.; Eddes, J. S.; et al. Mining a Tandem Mass Spectrometry Database to Determine the Trends and Global Factors Influencing Peptide Fragmentation. *Anal. Chem.* **2003,** *75,* 6251–6264.
22. Tabb, D. L.; Smith, L. L.; Breci, L. A.; et al. Statistical Characterization of Ion Trap Tandem Mass Spectra from Doubly Charged Tryptic Peptides. *Anal Chem* **2003,** *75,* 1155–1163.
23. Tabb, D. L.; Huang, Y. Y.; Wysocki, V. H.; Yates, J. R. Influence of Basic Residue Content on Fragment Ion Peak Intensities in Low-Energy—Collision-Induced Dissociation Spectra of Peptides. *Anal. Chem.* **2004,** *76,* 1243–1248.
24. Huang, Y. Y.; Triscari, J. M.; Pasa-Tolic, L.; et al. Dissociation Behavior of Doubly-Charged Tryptic Peptides: Correlation of Gas-Phase Cleavage Abundance with Ramachandran Plots. *J. Am. Chem. Soc.* **2004,** *126,* 3034–3035.

25. Ambihapathy, K.; Yalcin, T.; Leung, H. W.; Harrison, A. G. Pathways to Immonium Ions in the Fragmentation of Protonated Peptides. *J. Mass Spectrom.* **1997,** *32,* 209–215.
26. Nair, H.; Wysocki, V. H. Are Peptides without Basic Residues Protonated Primarily at the Amino Terminus? *Int. J. Mass Spectrom.* **1998,** *174,* 95–100.
27. Polce, M. J.; Ren, D.; Wesdemiotis, C. Special Feature: Commentary—Dissociation of the Peptide Bond in Protonated Peptides. *J. Mass Spectrom.* **2000,** *35,* 1391–1398.
28. Schlosser, A.; Lehmann, W. D. Special Feature: Commentary—Five-Membered Ring Formation in Unimolecular Reactions of Peptides: a Key Structural Element Controlling Low-Energy Collision-Induced Dissociation of Peptides. *J. Mass Spectrom.* **2000,** *35,* 1382–1390.
29. Salek, M.; Lehmann, W. D. Neutral Loss of Amino Acid Residues from Protonated Peptides in Collision-Induced Dissociation Generates N- or C-Terminal Sequence Ladders. *J. Mass Spectrom.* **2003,** *38,* 1143–1149.
30. Tsaprailis, G.; Nair, H.; Somogyi, A.; Wysocki, V. H.; et al. Influence of Secondary Structure on the Fragmentation of Protonated Peptides. *J. Am. Chem. Soc.* **1999,** *121,* 5142–5154.
31. Wysocki, V. H.; Tsaprailis, G.; Smith, L. L.; Breci, L. A. Special Feature: Commentary—Mobile and Localized Protons: A Framework for Understanding Peptide Dissociation. *J. Mass Spectrom.* **2000,** *35,* 1399–1406.
32. Yague, J.; Paradela, A.; Ramos, M.; et al. Peptide Rearrangement during Quadrupole Ion Trap Fragmentation: Added Complexity to MS/MS Spectra. *Anal. Chem.* **2003,** *75,* 1524–1535.
33. Grewal, R. N.; El Aribi, H.; Harrison, A. G.; et al. Fragmentation of Protonated Tripeptides: The Proline Effect Revisited. *J. Phys. Chem. B* **2004,** *108,* 4899–4908.
34. Gu, C. G.; Tsaprailis, G.; Breci, L.; Wysocki, V. H. Selective Gas-Phase Cleavage at the Peptide Bond Terminal to Aspartic Acid in Fixed-Charge Derivatives of Asp-Containing Peptides. *Anal. Chem.* **2000,** *72,* 5804–5813.
35. Tsaprailis, G.; Somogyi, A.; Nikolaev, E. N.; Wysocki, V. H. Refining the Model for Selective Cleavage at Acidic Residues in Arginine-Containing Protonated Peptides. *Int. J. Mass Spectrom.* **2000,** *196,* 467–479.
36. Wattenberg, A.; Organ, A. J.; Schneider, K.; et al. Sequence Dependent Fragmentation of Peptides Generated by MALDI Quadrupole Time-of-Flight (MALDI Q-TOF) Mass Spectrometry and Its Implications for Protein Identification. *J. Am. Soc. Mass Spectrom.* **2002,** *13,* 772–783.
37. Leymarie, N.; Berg, E. A.; McComb, M. E.; et al. Tandem Mass Spectrometry for Structural Characterization of Proline-Rich Proteins: Application to Salivary PRP-3. *Anal. Chem.* **2002,** *74,* 4124–4132.
38. Yu, W.; Vath, J. E.; Huberty, M. C.; Martin, S. A. Identification of the Facile Gas-Phase Cleavage of the Asp Pro and Asp Xxx Peptide-Bonds in Matrix-Assisted Laser-Desorption Time-of-Flight Mass-Spectrometry. *Anal Chem* **1993,** *65,* 3015–3023.
39. Burlet, O.; Yang, C. Y.; Gaskell, S. J. Influence of Cysteine to Cysteic Acid Oxidation on the Collision-Activated Decomposition of Protonated Peptides—Evidence for Intraionic Interactions. *J. Am. Soc. Mass Spectrom.* **1992,** *3,* 337–344.
40. Burlet, O.; Yang, C. Y.; Guyton, J. R.; Gaskell, S. J. Tandem Mass-Spectrometric Characterization of a Specific Cysteic Acid Residue in Oxidized Human Apoprotein B-100. *J. Am. Soc. Mass Spectrom.* **1995,** *6,* 242–247.
41. Qin, J.; Chait, B. T. Preferential Fragmentation of Protonated Gas-Phase Peptide Ions Adjacent to Acidic Amino-Acid-Residues. *J. Am. Chem. Soc.* **1995,** *117,* 5411–5412.
42. Summerfield, S. G.; Cox, K. A.; Gaskell, S. J. The Promotion of D-Type Ions during the Low Energy Collision-Induced Dissociation of Some Cysteic Acid-Containing Peptides. *J. Am. Soc. Mass Spectrom.* **1997,** *8,* 25–31.
43. Wang, Y. S.; Vivekananda, S.; Men, L. J.; Zhang, Q. B. Fragmentation of Protonated Ions of Peptides Containing Cysteine, Cysteine Sulfinic Acid, and Cysteine Sulfonic Acid. *J. Am. Soc. Mass Spectrom.* **2004,** *15,* 697–702.
44. Zhang, Z. Prediction of Low-Energy Collision-Induced Dissociation Spectra of Peptides. *Anal Chem.* **2004,** *76,* 3908–3922.
45. Huang, Y. Y.; Triscari, J. M.; Tseng, G. C.; et al. Statistical Characterization of the Charge State and Residue Dependence of Low Energy CID Peptide Dissociation Patterns. *Anal. Chem.* **2005,** in press.
46. Komaromi, I.; Somogyi, A.; Wysocki, V. H. Proton Migration and Its Effect on the MS Fragmentation of N-Acetyl OMe Proline: MS/MS Experiments and Ab Initio and Density Functional Calculations. *Int. J. Mass Spectrom.* **2005,** *241,* 315–323.
47. Reid, G. E.; Simpson, R. J.; O'Hair, R. A. J. A Mass Spectrometric and Ab Initio Study of the Pathways for Dehydration of Simple Glycine and Cysteine-Containing Peptide M+H (+) Ions. *J. Am. Soc. Mass Spectrom.* **1998,** *9,* 945–956.
48. Paizs, B.; Lendvay, G.; Vekey, K.; Suhai, S. Formation of b(2)(+) Ions from Protonated Peptides: An Ab Initio Study. *Rapid Commun. Mass Spectrom.* **1999,** *13,* 525–533.
49. Nold, M. J.; Wesdemiotis, C.; Yalcin, T.; Harrison, A. G. Amide Bone Dissociation in Protonated Peptides. Structures of the N-Terminal Ionic and Neutral Fragments. *Int. J. Mass Spectrom. Ion Process.* **1997,** *164,* 137–153.
50. Vaisar, T.; Urban, J. Low-Energy Collision Induced Dissociation of Protonated Peptides. Importance of an Oxazolone Formation for a Peptide Bond Cleavage. *Eur. Mass Spectrom.* **1998,** *4,* 359–364.
51. Vaisar, T.; Urban, J. Gas-Phase Fragmentation of Protonated Mono-N-Methylated Peptides. Analogy with Solution-Phase Acid-Catalyzed Hydrolysis. *J. Mass Spectrom.* **1998,** *33,* 505–524.
52. Harrison, A. G.; Csizmadia, I. G.; Tang, T. H. Structure and Fragmentation of b(2) Ions in Peptide Mass Spectra. *J. Am. Soc. Mass Spectrom.* **2000,** *11,* 427–436.
53. Wyttenbach, T.; Paizs, B.; Barran, P.; et al. The Effect of the Initial Water of Hydration on the Energetics, Structures, and H/D Exchange Mechanism of a Family of Pentapeptides: An Experimental and Theoretical Study. *J. Am. Chem. Soc.* **2003,** *125,* 13768–13775.
54. Campbell, S.; Rodgers, M. T.; Marzluff, E. M.; Beauchamp, J. L. Deuterium Exchange Reactions as a Probe of Biomolecule Structure. Fundamental Studies of Gas Phase H/D Exchange Reactions of Protonated Glycine Oligomers with D2O, CD3OD, CD3CO2D, and ND3. *J. Am. Chem. Soc.* **1995,** *117,* 12840–12854.
55. Gard, E.; Green, M. K.; Bregar, J.; Lebrilla, C. B. Gas-Phase Hydrogen/Deuterium Exchange as a Molecular Probe for the Interaction of Methanol and Protonated Peptides. *J. Am. Soc. Mass Spectrom.* **1994,** *5,* 623–631.
56. High Performance Computational Chemistry Group. NWChem, A Computational Chemistry Package for Parallel Computers; Pacific Northwest National Laboratory: Richland, WA, 2001.
57. Black, G. C., J.; Didier, B.; Feller, D.; Gracio, D.; Jones, D.; Keller, T.; Matsumoto, S.; Mendoza, E.; Olander, M.; Palmer, B.; Peden, N.; Schchardt, K.; Taylor, H.; Thomas, G.; Vorpagel, E.; Windus, T. Ecce, A Problem Solving Environment for Computational Software; 1.5 ed.; Pacific Northwest National Laboratory: Richland, WA 99352, 1999.
58. Dunning, T. H.; Hay, P. J. In *Methods of Electronic Structure Theory*; Schaefer, H. F., III, Ed.; Plenum Press: New York, 1977.

59. Magnusson, E.; Schaefer, H. F. Multiple D-Type Basis Functions for Molecules Containing 2nd Row Atoms. *J. Chem. Phys.* **1985,** *83,* 5721–5726.
60. Andzelm J.; et al. In Density Functional Methods in Chemistry; Labanowski, J., Andzelm, J., Eds.; Springer-Verlag: New York, 1991; pp 155.
61. Ziegler, T. Approximate Density Functional Theory as a Practical Tool in Molecular Energetics and Dynamics. *Chemical Reviews* **1991,** *91,* 651–667.
62. Becke, A. D. Density-Functional Thermochemistry. 3. The Role of Exact Exchange. *J. Chem. Phys.* **1993,** *98,* 5648–5652.
63. Lee, C.; Yang, W.; Parr, R. G. Development of the Colle-Salvetti Correlation-Energy Formula into a Functional of the Electron-Density. *Physical Review B* **1988,** *37,* 785–789.
64. Cieplak, P.; Cornell, W. D.; Bayly, C.; Kollman, P. A. Application of the Multimolecule and Multiconformational Resp Methodology to Biopolymers—Charge Derivation for DNA, RNA, and Proteins. *J. Computat. Chem.* **1995,** *16,* 1357–1377.
65. Bayly, C.; Cieplak, P.; Cornell, W. D.; Kollman, P. A. A Well-Behaved Electrostatic Potential Based Method Using Charge Restraints for Deriving Atomic Charges: The RESP Model. *J. Phys. Chem.* **1993,** *97,* 10269–10280.
66. Jiao, C. Q.; Ranatunga, D. R. A.; Vaughn, W. E.; Freiser, B. S. A Pulsed-Leak Valve for Use with Ion Trapping Mass Spectrometers. *J. Am. Soc. Mass Spectrom.* **1996,** *7,* 118–122.
67. Bartmess, J. E.; Georgiadis, R. M. Empirical-Methods for Determination of Ionization Gauge Relative Sensitivities for Different Gases. *Vacuum* **1983,** *33,* 149–153.
68. Gronert, S. Estimation of Effective Ion Temperatures in a Quadrupole Ion Trap. *J. Am. Soc. Mass Spectrom.* **1998,** *9,* 845–848.